Development 105, 17–25 (1989)
Printed in Great Britain © The Company of Biologists Limited 1989

Shaping and bending of the avian neural plate as analysed with a fluorescent–histochemical marker

GARY C. SCHOENWOLF and PHILIP SHEARD*

Department of Anatomy, University of Utah, School of Medicine, Salt Lake City, Utah 84132, USA

*Present address: Department of Physiology, University of Otago, Dunedin, New Zealand

Summary

Shaping and bending of the neural plate are cardinal events of neurulation. These processes are initiated in avian embryos shortly after the onset of gastrulation and concluded concomitantly with the completion of gastrulation. The epiblast undergoes extensive morphogenetic movements during gastrulation and neurulation, but the directions, distances, rates, mechanisms and roles of such rearrangements are largely unknown. To begin to understand these morphogenetic movements, we have mapped regional displacements of the epiblast by injecting a fluorescent–histochemical marker into selected prenodal, nodal and postnodal levels of the blastoderm. Lateral epiblast regions (600 μm lateral to the midline and consisting primarily of surface epithelium) are displaced craniomedially, medial regions (300 μm lateral to the midline and consisting of neural plate and preingressed mesoderm) predominantly medially, and midline regions (consisting of neural plate and primitive streak) predominantly caudally. Displacements within the avian neural plate parallel those previously described for the amphibian neural plate. Furthermore, similar tissue displacements occur within the prenodal and postnodal levels of the avian epiblast despite the fact that neurulation is occurring in the former and gastrulation in the latter. Finally, our results show that ectodermal rudiments contained within a single cross-sectional level of the embryo are a composite of cells derived from multiple craniocaudal and mediolateral levels. Thus, regional tissue displacements are important events to consider in the analysis of the early morphogenesis of axial and paraxial organ rudiments derived from the epiblast.

Key words: cell marker, chick embryo, gastrulation, neural plate, neurulation, R-HRP, peroxidase-rhodamine isothiocyanate.

Introduction

Development of the vertebrate embryo is characterized by a series of complex coordinated morphogenetic movements. These movements are initiated with gastrulation and continue throughout neurulation. Gastrulation movements centre on the primitive streak in avian embryos (reviewed by Nicolet, 1971; Vakaet, 1984). This structure is formed by epiblast cells that migrate toward the caudal midline of the area pellucida. The primitive streak extends cranially as cell accumulation occurs. Then, prospective endodermal and mesodermal cells migrate away from the streak and into the interior of the blastoderm where they form two of the three germ layers. By stage 4 (Hamburger & Hamilton, 1951), the primitive streak acquires its maximal length and its cranial end begins to move caudally.

Morphogenetic movements of gastrulation and neurulation are spatially and temporally coupled. The neural plate is induced by cells derived from the cranial end of the elongating primitive streak (Gallera, 1971). Neural plate shaping begins as mesodermal cells ingress through the cranial end of the primitive streak and the embryonic axis (the neural plate and notochord) extends caudally as Hensen's node (the cranial end of the primitive streak) regresses (Schoenwolf, 1982, 1985). Extension of the axis into the wake of the regressing node is accompanied by bending of the nascent neural plate, resulting in formation of the neural groove and the flanking neural folds. The latter fuse across the dorsal midline during subsequent development to form the neural tube. Streak regression and axis elongation continue until the streak is reduced to a small cluster of cells, the tail bud, at the caudal end of the blastoderm; the caudal neuropore closes in close proximity to the tail bud (Schoenwolf, 1979; Schoenwolf & DeLongo, 1980).

Little is known about the regional displacements of the epiblast occurring with, and largely constituting, the morphogenetic movements of gastrulation and neurulation. Previous fate-mapping studies on the avian blastoderm, using vital dyes, carbon marks or grafts of

cells labelled with tritiated thymidine, have delineated the boundaries of some of the major rudiments of the epiblast but have not analysed individual rudiments (e.g. Wetzel, 1929; Pasteels, 1937; Spratt, 1952; Rosenquist, 1966). It is important to map such displacements as a preliminary step in determining how early morphogenesis occurs. For example, temporal changes in cell shape and mitotic activity have been analysed in the avian neural plate (Schoenwolf & Franks, 1984; Smith & Schoenwolf, 1987, 1988). However, in the absence of mapping studies, it is impossible to determine whether these parameters were altered in the same population of cells or whether other populations with different parameters replaced previous ones. Burnside & Jacobson (1968) have mapped displacements within the neural plate of amphibian embryos by tracing movements of individual (or groups of) pigmented cells. Their results reveal that intricate displacement patterns occur within the amphibian neural plate during neurulation. Whether similar tissue displacements occur in higher vertebrates is unknown.

The purpose of the present study was to provide this missing information for the avian embryo, using a new technique: injection of a cell marker into discrete locations of the epiblast. This technique reveals that extensive tissue displacements occur within the epiblast during gastrulation and neurulation and provides quantitative data on their directions, distances and rates.

Materials and methods

Fertile White Leghorn chicken eggs were incubated in humidified incubators at 38°C for 12 to 19 h. Eggs were opened into bowls containing warm sterile saline (123 mM-NaCl), blastoderms were removed from the yolks and separated from the vitelline membranes, and embryos were staged. Embryos at stage 3 (Hamburger & Hamilton, 1951), were further classified into four substages – 3a, 3b, 3c, and 3d – according to the criteria of Vakaet (1962; stages 3a–3d represent, respectively, Vakaet's stages 3–6). Blastoderms were then cultured dorsal-side-up in Falcon plastic dishes (35×10 mm, Becton Dickinson Labware, Oxnard, California) on a substrate consisting of equal parts of egg albumen (mainly thin) and 0·6 % agar (Bacto-Agar; Difco, Detroit, MI) in 123 mM-NaCl (modification of the method of Spratt, 1947). A rim consisting of most of the area opaca was trimmed from each blastoderm prior to culturing, and excess saline was removed from the culture with a pipette. Cultures were incubated at 38°C and 95 % humidity.

Injection of the cell marker

Multiple injections of peroxidase–rhodamine isothiocyanate (R-HRP; made from type-VI peroxidase by Sigma Chemical Co., St Louis, no. P-5031; M_r ca. 40 000; 5 % w/v in sterile water) were made into different regions of the epiblast and displacement of the resulting fluorescent spots was followed over time (Figs 1, 2). An eyepiece reticle (demarcating 300 μm per grid side at ×25 magnification) mounted in a Wild stereomicroscope was used to identify each injection site, which was assigned a coordinate value. 4–23 injections were made into each epiblast at the level of Hensen's node (i.e. nodally – within the node or directly lateral to it), cranial to this level (i.e. prenodally) or caudal to this level (i.e. postnodally). Three mediolateral zones were injected, the midline (consisting of neural plate prenodally and Hensen's node and primitive streak postnodally), 300 μm lateral to the midline (consisting of neural plate prenodally and neural plate and preingressed mesoderm postnodally), and 600 μm lateral to the midline (consisting primarily of surface ectoderm) (Nicolet, 1971; Schoenwolf, 1985). Micropipettes were pulled from borosilicate glass capillary tubing (omega dot, 1·2 mm o.d., 0·6 mm i.d., catalog no. 30-31-1-075, Fred Haer and Co., Brunswick, Maryland) with a horizontal pipette puller. The tips were broken with fine forceps to give outside diameters of 8–12 μm, and pipettes were backfilled with R-HRP. Injections were made with the aid of an Eppendorf microinjector 5242 and a Narishige hydraulic micromanipulator. 0·5–1 nl of an R-HRP solution was injected at each site. A total of 115 embryos was injected; an additional 51 embryos served as uninjected controls.

Videomicroscopy and computer analysis

Cultures were examined with a Leitz epifluorescence microscope immediately after injection (designated 0 h) and illuminated for short intervals (less that 1 min) to avoid phototoxicity or bleaching of the label. Images were recorded and viewed with an MTI Dage ISIT 66 videocamera, a Panasonic AG 6010 videorecorder and a high resolution Panasonic colour monitor (CT-1400MG). Both bright-field and fluorescent images were videorecorded individually and simultaneously. Cultures were then reincubated. At selected intervals, ranging from 1 to 4 h, cultures were removed from the incubator, reexamined (again, they were illuminated for less than 1 min) and videotaped. Each culture was examined at four to six intervals (prenodal: 0 h, 1–3 h, 3–7 h, 7–10 h; postnodal: 0 h, 1–3 h, 3–5 h, 5–7 h, 7–11 h, 11–13 h), but the exact times at which viewing occurred during these intervals varied from specimen to specimen.

Images of the injection sites at each interval were digitized electronically from the videotape recordings and superimposed (see below) for computer analysis using a Sperry PC/IT computer (IBM PC/AT compatable) with Image-Pro image-analysis software (Media Cybernetics, Inc., Silver Spring, Maryland). Three parameters were assessed: rate of fluorescent spot displacement (μm h^{-1}), direction of displacement and regional changes in area. Directions of displacement were analysed by assigning each displacement an angular value with respect to a baseline drawn perpendicularly to the craniocaudal axis and passing through the initial injection site. For each side of the blastoderm, 0° was considered to lie on the baseline in the direction toward the median plane; 180° was considered to be directly lateral to this point. Displacements cranial to the baseline were assigned a positive value, and those caudal to the baseline, a negative value. Angles never exceeded 90°. Thus, positive or negative angles between 0° and 45° indicated movements predominantly medially, positive angles between 45° and 90° indicated movements predominantly cranially, and negative angles between 45° and 90° indicated movements predominantly caudally. Regional changes in area were assessed by using the computer to draw straight lines interconnecting adjacent digitized fluorescent spots at each interval and defining quadrilaterals. Surface areas demarcated by quadrilaterals were then calculated by the computer.

A midline injection placed 600 μm cranial to Hensen's node served as a fixed reference point for superimposing sequential images of the same embryo for analysis of prenodal regions. This point was the most stationary of any of those injected as determined from viewing time-lapse tapes (see below). Postnodal regions were analysed after prenodal regions. All

postnodal injection sites displaced extensively, so a fixed reference point could not be chosen. Instead, sequential digitized images were superimposed on the basis of the *expected* displacement of injections made directly lateral to Hensen's node. We had previously established the consistent displacement pattern of the nodal row from the results of the prenodal injections. Thus, we were able to use this knowledge in superimposing sequential time images of postnodal injections, configuring the displacement of the nodal row to be the same in both cases. As a result, all prenodal and postnodal displacements are given with respect to the fixed prenodal reference point.

Time-lapse videomicroscopy of control embryos also was used to examine epiblast displacements. The system consisted of a Panasonic AG 6050 time-lapse videocassette recorder with an external clock (allowing the recording of one frame every 12·5 s), an Hitachi videocamera with a Nuvicon tube, an Hitachi monitor, a Wild M-8 stereomicroscope and a temperature-controlled incubation chamber enclosing the microscope and the embryo culture during videotaping. The lid of the culture dish was sealed down with high vacuum grease (Dow Corning Corp., Midland, MI) to prevent dehydration. Cultures were taped continuously over 24 h. Ten videotapes were examined.

Histochemistry

Standard techniques were used to reveal the presence of HRP. Embryos were fixed at room temperature for 2 h with 1 % glutaraldehyde in 0·1 M-phosphate buffer at pH 7·2. They were then rinsed in the same buffer, placed in presoak solution containing 0·125 % diaminobenzidine tetrahydrochloride dihydrate (DAB) in buffer (0·1 M-phosphate at pH 7·2) for 1/2 h, transferred to a second solution of DAB containing hydrogen peroxide (0·075 %) for 1/2 h, washed with buffer and processed for paraffin histology using routine techniques. Sections were cut at 7 μm, mounted onto glass slides, and viewed unstained after dehydration, clearing and addition of coverslips.

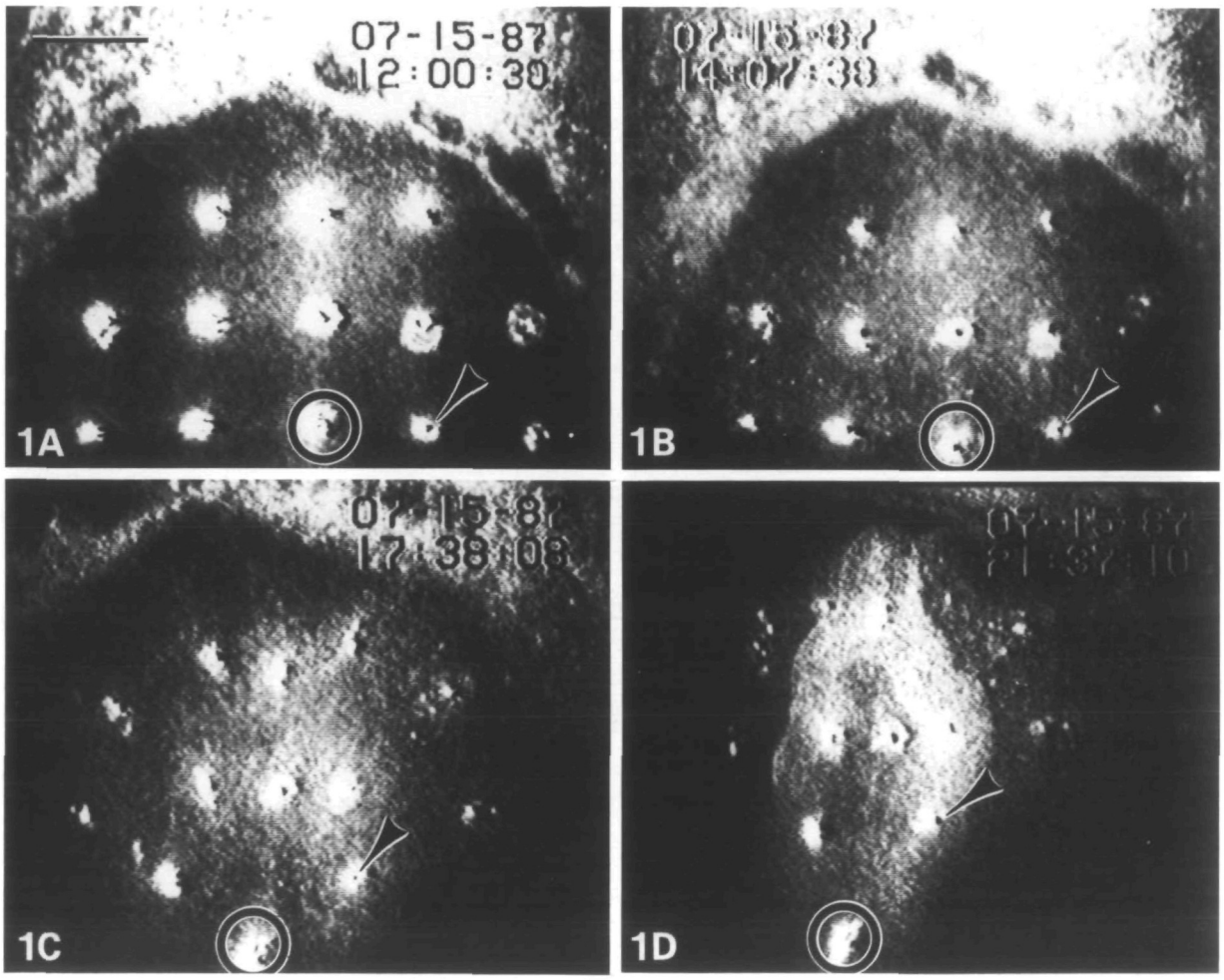

Fig. 1. Combined bright-field and fluorescent images recorded on videotape and photographed from the monitor's screen. Thirteen injection sites are visible in the prenodal and nodal levels of the epiblast at 0 h postinjection (A). The same sites are visible 2 h, 7 min (B), 5 h, 38 min (C) and 9 h, 37 min (D) postinjection. Injections were made within the midline, 300 μm lateral to the midline and 600 μm lateral to the midline. They were also made within the nodal row and prenodally, 300 and 600 μm cranial to the nodal row. Note that the sizes of the fluorescent patches decrease during the first interval due to diffusion from the injection site of excess label not confined within the epiblast. Hensen's node is encircled. Arrowheads mark the progress of a single injection site initially located 300 μm lateral to Hensen's node. Digitized images from this same blastoderm are shown in Fig. 5. Bar, 300 μm.

Results

Controls

Excellent development was obtained in cultured blastoderms. Neurulation seemed to have occurred normally in 92% of the control embryos. That is, a neural tube with normal morphology formed during the 24 h culture period. The only deviation from embryos developing *in ovo* concerned craniocaudal elongation, which was inhibited in culture. Thus, the rates and distances of fluorescent spot displacement in the *caudal* direction (described below) were likely underestimated. In the 8% of the cases where neurulation went awry, shaping of the neural plate seemed normal, but bending of the neural plate and closure of the neural groove were inhibited. Thus, only the more terminal events of neurulation were abnormal. A higher incidence of abnormal development was obtained when control embryos were removed periodically from the incubator (i.e. at the same intervals that experimental embryos were examined) than when they were incubated continuously (11% and 6%, respectively); this was probably due to partial dehydration of the albumen/agar substrate. Based on these control experiments, we would expect that 90–95% of our experimental embryos would neurulate normally. Experimental embryos that exhibited grossly retarded development were excluded from the data set.

Histochemistry

Paraffin sections of control and injected embryos were examined for peroxidase reaction product to determine the location of the injected material within the epiblast. (Fluorescence could not be detected in *sections* because of tissue autofluorescence; also fluorescence was short-lived.) Control embryos lacked reaction product (Fig. 3A), whereas localized reaction product was present in many of the injection sites of experimental embryos. Completely labelled cells were present in about one-third of the positive injection sites examined (Fig. 3B). In the remaining positive injection sites, a particulate 'cloud' of reaction product was identifiable (Fig. 3C). It could not be determined from our light micrographs whether individual particles were intercellular or intracellular.

Fluorescent spot displacements

Fluorescent spots, followed in intact embryos over time (see following sections), showed similar rates, directions and distances of displacement. Individual fluorescent spots occasionally split into two spots, each of which was about half the size of the original spot. Pairs of spots (presumably daughter cells) remained near to one another during subsequent displacement.

Prenodal epiblast displacements

13 of the 77 blastoderms injected both prenodally and nodally were selected for detailed analyses based mainly on the following criteria, normality of development, quality of the injection (i.e. whether fluorescent spots remained visible), number of injection sites and locations of the injection sites. Many other blastoderms, which received some successful injections, were omitted from the data set to prevent it from becoming unmanageable.

The following displacements were identified in all embryos examined regardless of their stage (Figs 4, 5). (1) The most laterally marked region of the epiblast (i.e. the area containing marks located 600 μm lateral to

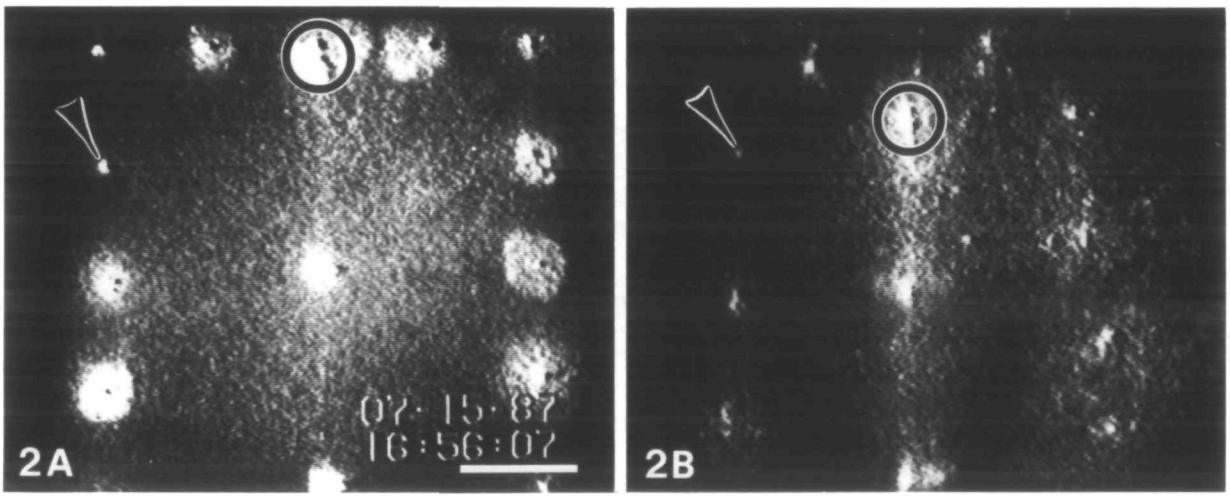

Fig. 2. Combined bright-field and fluorescent images recorded on videotape and photographed from the monitor's screen. Fifteen injection sites are visible in the postnodal and nodal levels of the epiblast at 0 h postinjection (A). The same sites are present at 5 h, 50 min postinjection (B); however, some spots have moved out of the field of view. Injections in the nodal row were made within the midline, 300 μm lateral to the midline and 600 μm lateral to the midline. Postnodal injections within the midline were made 600 and 1200 μm caudal to the nodal row. Postnodal injections 600 μm lateral to the midline were made 300, 600, 900 and 1200 μm caudal to the nodal row. Hensen's node is encircled. Arrowheads mark the progress of a single injection site initially located 600 μm lateral and 300 μm caudal to Hensen's node. Digitized images from this same blastoderm are shown in Fig. 9 (A,C). Bar, 300 μm.

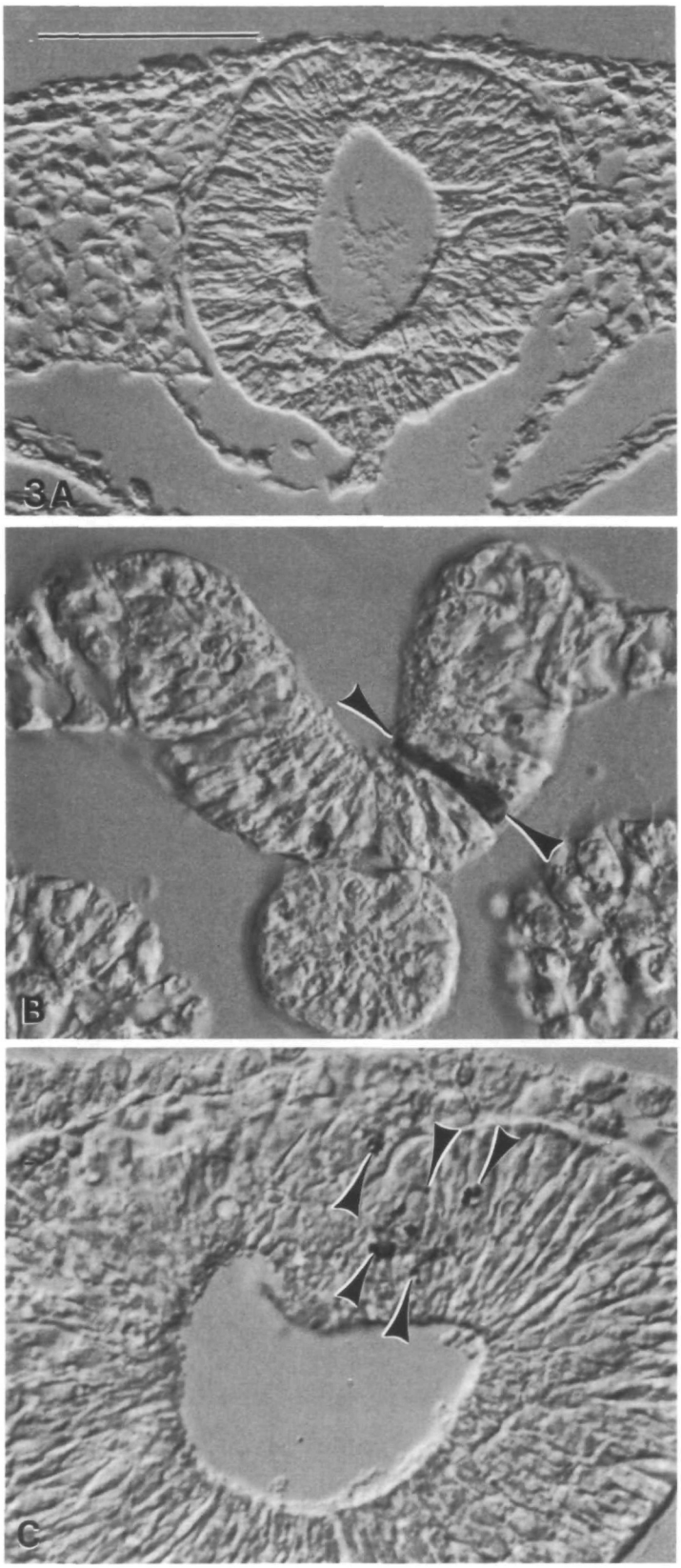

Fig. 3. Paraffin sections, viewed with differential–interference–contrast optics, of control (A) or R-HRP-injected (B,C) blastoderms fixed 24 h postinjection. In A (hindbrain level), note the lack of peroxidase reaction product. In B (spinal cord level), a single neuroepithelial cell is completely labelled (arrowheads). In C (midbrain level, dorsal part of neural tube), a particulate cloud of reaction product is present (arrowheads indicate some of the scattered peroxidase-positive particles). Bar, 100 μm (A) and 50 μm (B,C).

the midline) was displaced craniomedially (average value of 57°) at an average rate of 62 μm h^{-1}. Time-lapse videomicroscopy of control embryos revealed that the width of the area pellucida decreased and its length increased as these displacements occurred. Thus, the shape of the area pellucida changed from circular to oval. (2) The medial region flanking the midline (i.e. 300 μm lateral to it) was displaced predominantly medially but also somewhat cranially (average value of 26°). This region was displaced at an average rate of 29 μm h^{-1}. (3) The midline region was displaced predominantly caudally at an average rate of 24 μm h^{-1}. Time-lapse videomicroscopy of control embryos revealed that displacement cranially also occurred in the midline during late stages of neurulation when the forebrain and head fold of the body were forming.

By means of the image analysis program, we were able to join adjacent digitized fluorescent spots with straight lines and accurately measure the areas of the resulting prenodal quadrilaterals. We found these areas to decrease as gastrulation and neurulation progressed, irrespective of the particular quadrilateral examined (average decrease of 31 % over 10 h) (Figs 5, 6). Decrease in area was the result of a reduction in the width of each quadrilateral with a less than compensating increase in its length.

Postnodal epiblast displacements

11 of the 38 blastoderms injected both postnodally and nodally were chosen for detailed analysis based on the same criteria used for the prenodal areas.

The following displacements were identified in all

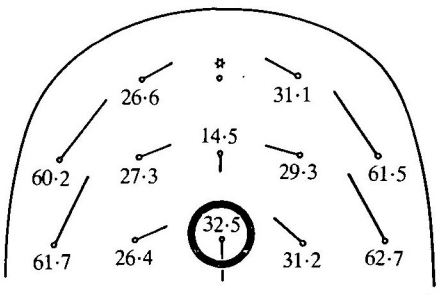

Fig. 4. Drawing showing average changes in positions of 13 prenodal and nodal epiblast injection sites over a 10 h period. The site 600 μm cranial to Hensen's node (asterisk) was chosen as a fixed reference point. The length of each line indicates the average distance of displacement (the end of each line marked with a dot indicates the initial injection site), the orientation of each line indicates the direction of displacement and the number next to each point indicates the rate of displacement (μm h^{-1}). The initial position of Hensen's node is encircled. Bar, 300 μm.

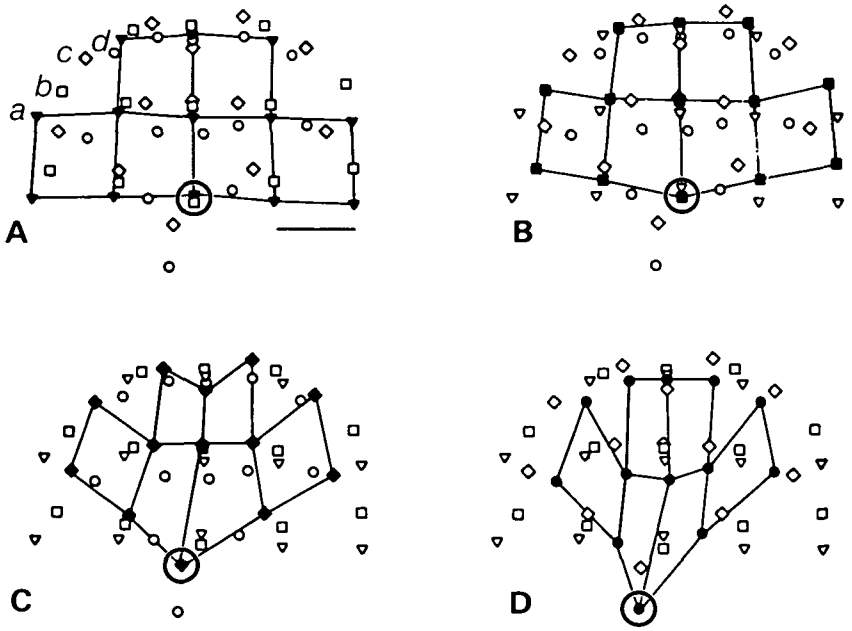

Fig. 5. Superimposed digitized images from four intervals of the blastoderm shown in Fig. 1. Letters *a–d* (and, respectively, symbols ▽, □, ◇, ○) indicate four positions of the same site at the intervals depicted in the correspondingly labelled figures. A filled symbol is used in each frame to indicate adjacent injection sites interconnected by straight lines. In A, straight lines have been drawn to interconnect the initial positions of the adjacent injection sites. In B–D, the lines interconnect adjacent sites at three intervals postinjection (B: 2 h, 7 min; C: 5 h, 38 min; and D: 9 h, 37 min). Sites have new positions at each interval. Hensen's node is encircled. Bar, 300 μm.

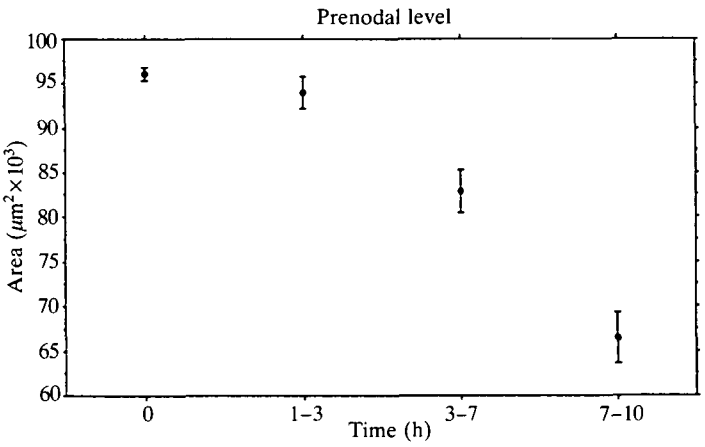

Fig. 6. Graph showing changes in average quadrilateral surface areas (±S.E.M.) from the prenodal level at the time of injection and at three intervals thereafter. Six to eight quadrilaterals (example showing six, illustrated in Fig. 5), initially squares with approximately 300 μm sides, were analysed in each embryo.

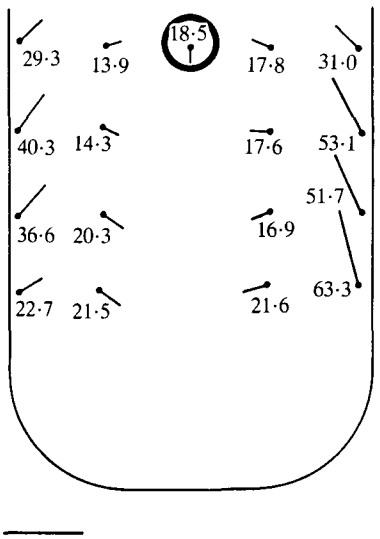

Fig. 7. Drawing showing average changes in positions of 17 postnodal and nodal epiblast injections over a 13 h period. The length of each line indicates the average distance of displacement (the end of each line marked with a dot indicates the initial injection site), the orientation of each line indicates the direction of displacement and the number next to each point indicates the rate of displacement ($\mu m\,h^{-1}$). The initial position of Hensen's node is encircled. Bar, 300 μm.

embryos examined regardless of their stage (Figs 7–9). (1) The most-laterally marked region of the epiblast (i.e. 600 μm lateral to the primitive streak) was displaced predominantly cranially but also medially (average value of 53°). This region was displaced at an average rate of 41 $\mu m\,h^{-1}$. (2) The medial region flanking the primitive streak (i.e. 300 μm lateral to it) was displaced predominantly medially (average value of −12°). The precise direction of displacement of this region was variable. On the average, the cranial end of this region was displaced cranially, its caudal end, caudally, and the area in between, directly medially. Overall, the medial region was displaced at an average rate of 18 $\mu m\,h^{-1}$. (3) The midline region (i.e. within the primitive streak) was displaced either caudally or cranially depending on the craniocaudal level. The cranial end of the streak (including Hensen's node) was displaced caudally, while the caudal end of the streak (including the nodus posterior) was displaced cranially. Thus, the primitive streak shortened as a result of a bidirectional movement. This shortening occurred at an average rate of 19 $\mu m\,h^{-1}$

The same analysis of change in area of quadrilaterals formed by joining digitized fluorescent spots as described for prenodal regions was performed also for postnodal regions. As in prenodal regions, the area of

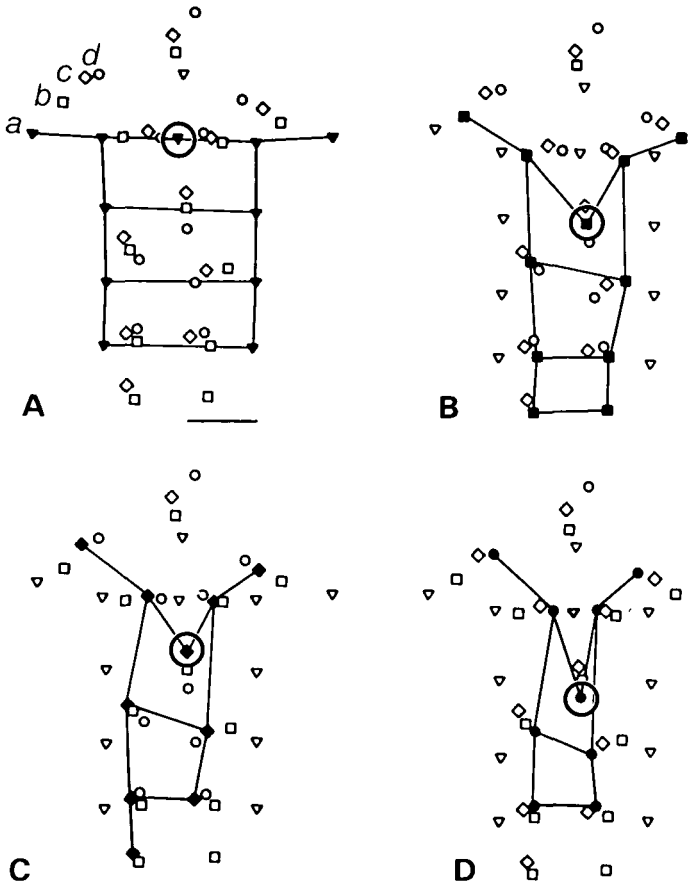

Fig. 8. Superimposed digitized images from four intervals of a blastoderm injected postnodally and nodally. Injections in the nodal row were made within the midline, 300 μm lateral to the midline and 600 μm lateral to the midline. Postnodal injections were made 300 μm lateral to the midline. They were also made 300, 600 and 900 μm caudal to the nodal row. Letters *a–d* (and, respectively, symbols ∇, $\square$, $\diamond$, $\bigcirc$) indicate four positions of the same site at the intervals depicted in the correspondingly labelled figures. A filled symbol is used in each frame to indicate adjacent injection sites interconnected by straight lines. In A, straight lines have been drawn to interconnect the initial positions of several of the adjacent injection sites. In B–D, the lines interconnect adjacent sites at three intervals postinjection (B: 7 h, 12 min; C: 9 h, 4 min; and D: 11 h, 10 min). Sites have new positions at each interval. Hensen's node is encircled. Bar, 300 μm.

each postnodal quadrilateral decreased, due to a decrease in each quadrilateral's width and a less than compensating increase in its length (average decrease of 34 % over 13 h) (Figs 8–10).

Discussion

Localized displacement of an epithelial sheet such as the avian epiblast could occur by various mechanisms. Changes in cell position within the epithelium by cell migration, either in unison (i.e. within a cell stream) or individually (i.e. with change in cell neighbours) is, perhaps, the most obvious possibility. However, cell position also could be altered by localized changes in cell number (due to cell division, cell intercalation from adjacent tissues or changes in the density of cell packing), cell shape or cell size. Furthermore, the situation is complicated by the likelihood that forces for displacement could be generated actively, by cells within the displacing region of the epithelium, or passively, by cells outside this area. In the latter case, displacement could be the result of a 'flow' of cells into a path of least resistance. These possibilities cannot be evaluated by the methods used in the present study. Rather, the purpose of this study was to elucidate precisely the magnitude and direction of cell displacements as a prelude to determining how they occur and their roles in axial morphogenesis.

One technical issue first needs to be discussed to aid in the evaluation of the results: the degree of normalcy of development in culture. The use of culture was necessary to obtain direct access to the epiblast. A modified Spratt (1947) culture was used rather than the more conventional New (1955) culture because, in the latter, only the ventral surface of the blastoderm is directly accessible. Centrifugal expansion of the blastoderm occurs better in New culture than in Spratt culture (New, 1966), but this is unlikely to affect our results since fluorescent spots generally were placed centrally within the blastoderm rather than near its perimeter.

One important morphogenetic movement was clearly inhibited in culture: axis elongation. Tissue displacement in the prenodal midline occurred at the rate of 24 $\mu m\,h^{-1}$, or 240 μm over a 10 h period. Previous studies, based on living or sectioned material, suggest this rate should be greater (Jacobson, 1978, 1980, 1981, 1984; Schoenwolf, 1985). Thus, although the direction of displacement of midline cells could be resolved accurately with the techniques used in the present study, the rate of displacement of these cells should be considered underestimated. Inhibition of axis elongation probably accounts for the observed decrease in prenodal quadrilateral surface areas. Recall that the width of each quadrilateral decreased while its length increased. Our morphometric studies, based on embryos developing *in ovo*, have shown that the width of the neural plate also decreases during shaping while its length increases (Schoenwolf, 1985). The length increase is several times greater than the width decrease so that neural plate surface area increases.

The rates of other morphogenetic movements apparently were not inhibited in culture. For example, medial prenodal regions (i.e. 300 μm lateral to the midline and consisting of neural plate; see below) displaced at the rate of 29 $\mu m\,h^{-1}$, or 290 μm over a 10 h period. This would result in halving of the width of the neural plate during this period, which corresponds to the results of our morphometric study (Schoenwolf, 1985).

In the present study, the directions, rates and distances of tissue displacements were mapped in three mediolateral zones of the epiblast. Aside from determining the magnitude of tissue displacements, three major findings were obtained. First, tissue displacement

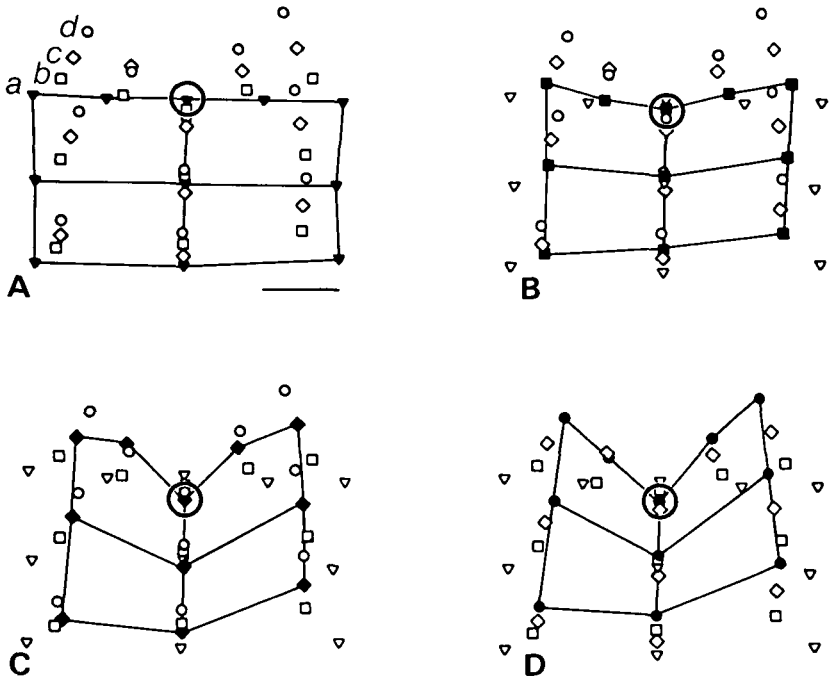

Fig. 9. Superimposed digitized images from four intervals of the blastoderm shown in Fig. 2. Letters *a–d* (and, respectively, symbols ▽, □, ◇, ○) indicate four positions of the same site at the intervals depicted in the correspondingly labelled figures. A filled symbol is used in each frame to indicate adjacent injection sites interconnected by straight lines. In A, straight lines have been drawn to interconnect the initial positions of several of the adjacent injection sites. In B–D, the lines interconnect adjacent sites at three intervals postinjection (B: 3 h, 44 min; C: 5 h, 50 min; and D: 7 h, 48 min). Sites have new positions at each interval. Hensen's node is encircled. Bar, 300 μm.

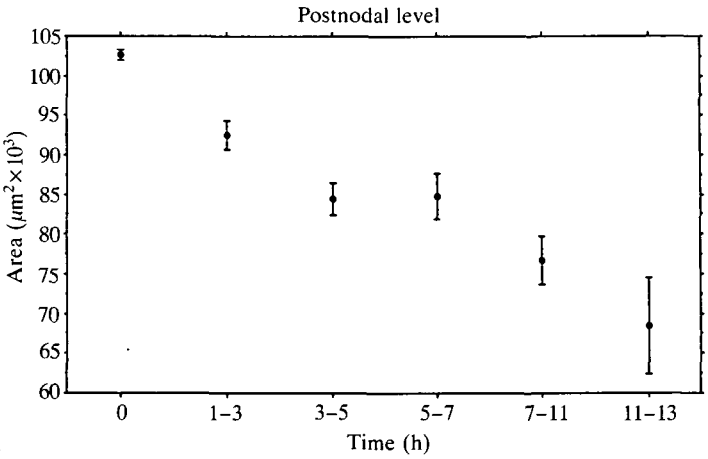

Fig. 10. Graph showing changes in average quadrilateral surface areas (±S.E.M.) from the postnodal level at the time of injection and at five intervals thereafter. Six to twelve quadrilaterals were analysed in each embryo. In the example shown in Fig. 8, initially three rectangles (300×600 μm) were drawn. Midline points were not available. Thus, to facilitate comparisons between prenodal and postnodal levels, each initial rectangle was considered as being bisected into two squares with approximately 300 μm sides, and six quadrilaterals were analysed over time. Similarly, in the example shown in Fig. 9, points 300 μm lateral to the streak were not available. Therefore, each initial rectangle was considered as being bisected into two squares with approximately 300 μm sides, and eight quadrilaterals were analysed over time.

within the prospective and definitive neural plate of avian embryos is similar to that occurring within the neural plate of amphibian embryos (Burnside & Jacobson, 1968). In both types of embryos, midline neural plate is displaced caudally while lateral neural plate is displaced medially and cranially. Second, similar displacements occur within each zone regardless of whether the mark was placed prenodally, nodally or postnodally. On the surface, this finding seems surprising because different developmental processes occur cranial and caudal to Hensen's node (i.e. neurulation and gastrulation, respectively) and somewhat different rudiments occupy these levels (neural plate and surface ectoderm prenodally, and neural plate, preingressed mesoderm and surface ectoderm postnodally). However, in actuality, similar events occur both prenodally and postnodally (Nicolet, 1971; Schoenwolf, 1985). For example, neurulation involves the craniocaudal elongation of the neural plate (so the prenodal midline is displaced caudally), and gastrulation involves regression of Hensen's node and the cranial part of the primitive streak (so the nodal and postnodal midline moves caudally). In addition, neurulation involves narrowing of the neural plate and convergence of the neural folds (so prenodal marks placed 300 μm lateral to the midline are displaced medially) and gastrulation involves migration of epiblast cells toward the primitive streak where they ingress (so postnodal marks placed 300 μm lateral to the midline are displaced medially). Finally, time-lapse videomicroscopy from the present study revealed that during the period of analysis, the area pellucida elongated craniocaudally. Thus, cranial displacement of both prenodal and postnodal marks placed 600 μm lateral to the midline (and presumably labelling cells in the surface epithelium) reflect this event.

The third major finding of this study is that adjacent marks in different mediolateral zones are displaced in different directions. Therefore, ectodermal rudiments in single, cross-sectional levels of the embryo are a composite of epiblast cells derived from multiple mediolateral and craniocaudal levels. For example, at the hindbrain level of the recently formed neural tube,

the ventral midline of the neural tube (i.e. its floor plate) is derived from cells originating in the midline more cranially, its lateral walls from cells originating more laterally and its surface epithelial covering from cells originating more caudolaterally. Such tissue displacements occurring during the formation of axial and paraxial organ rudiments are important to consider when analysing morphogenetic mechanisms. Apparently, they are not unique to avian embryos because the previous mapping studies of Burnside & Jacobson (1968) suggest similar displacements occur in the amphibian neural plate.

In summary, our results using a new technique delineate tissue displacements occurring within the avian epiblast during gastrulation and neurulation. Data on the directions, distances and rates of displacement are provided. These results extend those previously obtained by other methods on amphibian embryos and provide an initial step for determining how tissue displacements occur in higher vertebrates in which growth is an important factor in morphogenesis.

Technical assistance was provided by Nancy Chandler, Maggie Kasten and Jodi Smith, and secretarial assistance by Brenda Sahr. This research was supported by NIH grant no. NS 18112 and was conducted in part using facilities from the laboratory of Professor Marcus Jacobson. His generosity and kindness in support of this study are gratefully acknowledged.

References

BURNSIDE, M. B. & JACOBSON, A. G. (1968). Analysis of morphogenetic movements in the neural plate of the newt *Taricha torosa*. *Devl Biol.* **18**, 537–552.

GALLERA, J. (1971). Primary induction in birds. *Adv. Morph.* **9**, 149–180.

HAMBURGER, V. & HAMILTON, H. L. (1951). A series of normal stages in the development of the chick embryo. *J. Morph.* **88**, 49–92.

JACOBSON, A. G. (1978). Some forces that shape the nervous system. *Zoon* **6**, 13–21.

JACOBSON, A. G. (1980). Computer modeling of morphogenesis. *Am. Zool.* **20**, 669–677.

JACOBSON, A. G. (1981). Morphogenesis of the neural plate and tube. In *Morphogenesis and Pattern Formation* (ed. T. G. Connelly, L. L. Brinkley & B. M. Carlson), pp. 233–263. New York: Raven Press.

JACOBSON, A. G. (1984). Further evidence that formation of the neural tube requires elongation of the nervous system. *J. exp. Zool.* **230**, 23–28.

NEW, D. A. T. (1955). A new technique for the cultivation of the chick embryo *in vitro*. *J. Embryol. exp. Morph.* **3**, 320–331.

NEW, D. A. T. (1966). *The Culture of Vertebrate Embryos*, pp. 47–98. London: Logos Press.

NICOLET, G. (1971). Avian gastrulation. *Adv. Morph.* **9**, 231–262.

PASTEELS, J. (1937). Etudes sur la gastrulation des vertébrés méroblastiques. III. Oiseaux. IV. Conclusions générales. *Archs Biol.* **48**, 381–488.

ROSENQUIST, G. C. (1966). A radioautographic study of labeled grafts in the chick blastoderm. Development from primitive-streak stages to stage 12. *Contrib. Embryol.* **38**, 73–110.

SCHOENWOLF, G. C. (1979). Observations on closure of the neuropores in the chick embryo. *Am. J. Anat.* **155**, 445–466.

SCHOENWOLF, G. C. (1982). On the morphogenesis of the early rudiments of the developing central nervous system. *Scanning Electron Microsc.* 1982(I), 289–308.

SCHOENWOLF, G. C. (1985). Shaping and bending of the avian neuroepithelium, Morphometric analyses. *Devl Biol.* **109**, 127–139.

SCHOENWOLF, G. C. & DELONGO, J. (1980). Ultrastructure of secondary neurulation in the chick embryo. *Am. J. Anat.* **158**, 43–63.

SCHOENWOLF, G. C. & FRANKS, M. V. (1984). Quantitative analyses of changes in cell shapes during bending of the avian neural plate. *Devl Biol.* **105**, 257–272.

SMITH, J. L. & SCHOENWOLF, G. C. (1987). Cell cycle and neuroepithelial cell shape during bending of the chick neural plate. *Anat. Rec.* **218**, 196–206.

SMITH, J. L. & SCHOENWOLF, G. C. (1988). Role of cell cycle in regulating neuroepithelial cell shape during bending of the chick neural plate. *Cell Tiss. Res.* **252**, 491–500.

SPRATT, N. T., JR (1947). A simple method for explanting and cultivating early chick embryos *in vitro*. *Science* **106**, 452.

SPRATT, N. T., JR (1952). Localization of the prospective neural plate in the early chick blastoderm. *J. exp. Zool.* **120**, 109–130.

VAKAET, L. (1962). Some new data concerning the formation of the definitive endoblast in the chick embryo. *J. Embryol. exp. Morph.* **10**, 38–57.

VAKAET, L. (1984). Early development of birds. In *Chimeras in Developmental Biology* (ed. N. LeDouarin & A. McLaren), pp. 71–88. London: Academic Press.

WETZEL, R. (1929). Untersuchungen am hühnchen. Die entwicklung des keims während der ersten beiden bruttage. *Wilhelm Roux' Arch. EntwMech. Org.* **119**, 188–321.

(*Accepted 20 September 1988*)